Preprints of the 21st IFAC World Congress (Virtual)
Berlin, Germany, July 12-17, 2020

Nanoforce Estimation using Interval Observer: Application to Force Sensor based on Diamagnetic Levitation ⋆

Fawzia Amokrane * **Adrien Drouot** * **Joël Abadie** *
Emmanuel Piat *

* *FEMTO-ST Institute, Univ. Bourgogne Franche-Comté, CNRS, 15B avenue des Montboucons, 25030 Besançon, cedex, France, (e-mail: {fawzia.amokrane, adrien.drouot, joel.abadie}@femto-st.fr, emmanuel.piat@ens2m.fr)*

Abstract: This paper presents a new design to measure slowly time-varying vertical nanoforces. The proposed sensor is based on diamagnetic levitation. It uses auto-stabilized magnetic springs and relies on a macroscopic seismic mass: a capillary tube used in a vertical configuration. When a vertical external force is applied to it, the capillary tube acts as a transducer that converts this unknown input force into a vertical displacement that is measured. Relying on this measurement, a Generic Linear Extended State Observer based on an interval approach is proposed to reconstruct this unknown input force and the state of the considered system. This is achieved without any a priori knowledge on the vertical force, i.e. magnitude and bounds. The efficiency of the proposed interval observer is illustrated by experimental results.

Keywords: Nanoforce sensors, Interval observers, LTI systems.

1. INTRODUCTION

Achieving headway in the field of micro and nano forces measurement remains essential in several fields like micromanipulation and microassembly, materials science at micro and nano scales or micro and nanorobotics. Such progresses rely essentially on the force sensors, whose design is constrained by the fact that only the force effects can be directly measured. That is why a sensitive part, called transducer, is needed to convert the force into a physical effect that can be measured using different technologies.

The literature gives examples of such microforces measurement technologies. One can find piezoresistive sensors that rely on the variation of the piezoresistive layer resistance when a force is applied (Estevez et al., 2012; Billot et al., 2015), capacitive sensors that are based on the changes in capacitance between two electrodes when their distance changes during force application (Beyeler et al., 2009) and piezoelectric sensors which generate a voltage when they are stressed (Shen et al., 2003). There are also examples of nanoforces measurement technologies such as sensors using auto-stabilized magnetic springs associated to a macroscopic seismic mass (in the milligram to gram range). When an unknown force is applied to the macroscopic seismic mass, the latter acts as a transducer that converts this unknown input into a displacement that is measured (Piat et al., 2012; Billot et al., 2016). This technology has been successfully used in the last decade to design different nanoforces measurement platforms, for instance to achieve the mechanical characterization of biological cells like human oocytes (Gana et al., 2017).

⋆ This work has been supported by the EIPHI Graduate school (contract "ANR-17-EURE-0002").

Among the sensors using auto-stabilized magnetic springs, passive diamagnetic levitation-based force sensors are known for their low resonant frequency and their low stiffness. Moreover, the manufacturing of the mechanical part is a low-cost processing that does not necessitate any complex machining, thanks to the macroscopic size of the transducer (levitating mass). However, their main disadvantage is their limited bandwidth.

In this particular technology, the applied force is considered as an unknown input and its effect is the displacement of the macroscopic seismic mass that can be measured using an appropriate displacement sensor. The applied force is then reconstructed using an observer like the Unknown Input Observer (UIO) (Hou and Muller, 1992), the extended-state linear Kalman Filter (Piat et al., 2012), etc. These approaches are model-based techniques.

In order to deal with the unavoidable uncertainties associated with the sensor modeling, the development of interval observers (Gouzé et al., 2000) represents an alternative technique for robust estimation in presence of uncertainties. The goal of this approach consists in providing a guaranteed lower and upper bounds covering all the admissible trajectories of the system at any time. The design of these observers requires a condition of cooperativity of the interval estimation error dynamics. This condition preserves the order relationship between lower and upper trajectories (Mazenc and Bernard, 2011). However, searching for a qualified observer gain ensuring the cooperativity condition is not a trivial task and is sometimes impossible. To overcome this difficulty, the cooperativity condition is relaxed for LTI systems using a time-invariant change of coordinates that is obtained by solving a Sylvester equation (Raissi et al., 2012) or by running nonsmooth

optimization techniques (Chambon et al., 2015). The cooperativity condition can also be relaxed using a time-varying change of coordinates (Mazenc and Bernard, 2011).

In this paper, an interval observer is used to estimate the lower and the upper bound of both the state and unknown external force acting on the nanoforce sensor. It is based on the Generic Linear Extended State Observer (GeLESO) developed by Amokrane et al. (2019), where an extended state is introduced. The dynamics of this extended state depends on the external force dynamics, i.e. it depends on the external force derivative. The advantage of the proposed approach is that it does not necessitate to specify any a priori bounds on the external force derivative to compute the bounds of the external force at any time. This observation scheme will be used alongside a new sensor design based on auto-stabilized magnetic springs associated to a macroscopic seismic mass in order to measure slowly time-varying vertical nanoforces.

The remainder of the paper is organized as follows. Some preliminaries are given in section 2. Section 3 introduces the nanoforce sensor, i.e. its design, principle and modelling. Section 4 presents the interval observer designed to estimate the state of the system and the unknown external force acting on it. The experimental results are provided in section 5. Finally, the conclusion is given in section 6.

2. PRELIMINARIES

In this section, some useful lemmas, notations and basic definitions used throughout this paper are introduced.

Note that all the inequalities must be interpreted element-wise.

For all vector $x \in R^n$, $|x|$ is the element-wise absolute value of x. $\overline{x}$ and $\underline{x}$ represent respectively the upper and lower bound of x, where $\underline{x} \leq x \leq \overline{x}$.

For all matrix $A \in R^{n\times n}$, $A^+ = \max\{0, A\}$ and $A^- = A^+ - A$.

Definition 1. A matrix $A = (a_{ij})$ is called a Metzler matrix if $a_{ij} \geq 0, \forall\, i \neq j$.

Definition 2. A continuous-time linear system is a cooperative system, if its state matrix A is a Metzler matrix.

Lemma 1. (Efimov et al., 2012)
Let $x \in R^n$ be a vector variable, $\underline{x} \leq x \leq \overline{x}$ for some $\underline{x}$, $\overline{x} \in R^n$. For a constant matrix $A \in R^{m\times n}$

$$A^+\underline{x} - A^-\overline{x} \;\leq\; Ax \;\leq\; A^+\overline{x} - A^-\underline{x}. \tag{1}$$

Lemma 2. (Gouzé et al., 2000)
For a Metzler matrix A, the linear system

$$\dot{x}(t) = Ax(t) + \alpha, \tag{2}$$

with $x \in R^n$ and $\alpha \geq 0$, is said to be cooperative if A is Metzler. Then for any initial conditions $x(0) \geq 0$, we have $x(t) \geq 0, \forall\, t \geq 0$.

3. VERTICAL NANOFORCE SENSOR BASED ON DIAMAGNETIC LEVITATION

3.1 Sensor description

Nanoforce sensors based on auto-stabilized magnetic springs are characterized by their low resonant frequency. They are associated with a macroscopic seismic mass (in the milligram to gram range) that interacts with the magnetic springs. They are known to be an alternative to classical designs (AFM, piezoresistive force sensors, etc.) to measure low frequency forces or quasi static forces.

Cherry et al. (2011) presented a force sensor based on magnetic springs and stabilized by upthrust buoyancy. The seismic mass of 4 g is a float with a magnet. Its resolution is around 10 nN and its measurement range is $\pm$ 50 μN. This force sensor can measure the horizontal component of an external force and the vertical component of an external torque. Piat et al. (2012) presented another force sensor based on magnetic springs. It is based on a macroscopic mass ($\simeq$ 70 mg) that is levitating passively thanks to the diamagnetic levitation principle. This mass is a rigid 10 cm long horizontal capillary tube made of glass to which are stuck two small magnets. This sensor uses repulsive diamagnetic force (Boukallel et al., 2003) instead of repulsive upthrust buoyancy to stabilize the seismic mass.

In this paper a new nanoforce sensor based on diamagnetic levitation is presented. This nanoforce sensor is designed to measure vertical forces, whereas the two previous ones measure only horizontal forces. The seismic mass is a 2 cm long capillary tube made of glass to which is attached a cylindrical magnet M of 1 $\times$ 1 mm (see figure 1) weighing around 8 mg in total. It levitates vertically around a given equilibrium state thanks to the repulsive diamagnetic forces generated by four graphite diamagnetic plates, coupled with attractive magnetic forces generated by two coils (see figure 2). The current i circulating in the coils allows to adjust the levitation height of the magnet M. As long as the magnet stays between the diamagnetic plates, the position of the capillary tube remains stable for any current i.

The levitating capillary tube is used as a vertical force sensing device along axis $\boldsymbol{z}$. It is designed to measure the external force $\overrightarrow{F_d}$. The vertical displacement of the capillary tube induced by the external force is measured using a confocal chromatic sensor (PRECITEC, optical probe with a 300 μm range). The whole structure is placed inside a climatic chamber (Kambič PKK-125) located on an anti-vibration table. The structure of the force sensor is shown in figure 3.

3.2 Modeling and force sensing principle

The dynamics of the capillary tube is characterized by a second order linear ODE. It is linear for vertical displacements in a range of $\pm$ 20 μm around its operating point, and it can measure forces between 1 nN and 1 μN.

The forces involved in the levitating tube dynamics along the $\boldsymbol{z}$ axis are: its weight, the unknown external force $\overrightarrow{F_d}$, the electromagnetic force $\overrightarrow{F_{elec}}$ generated by the electromagnets E^m and the viscous friction due to the

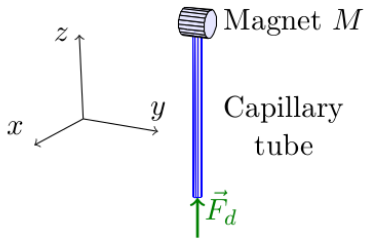

Fig. 1. Macroscopic seismic mass (capillary tube)

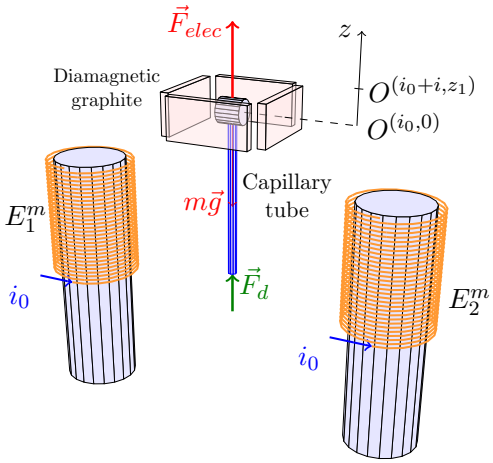

Fig. 2. Capillary tube in the force sensing device

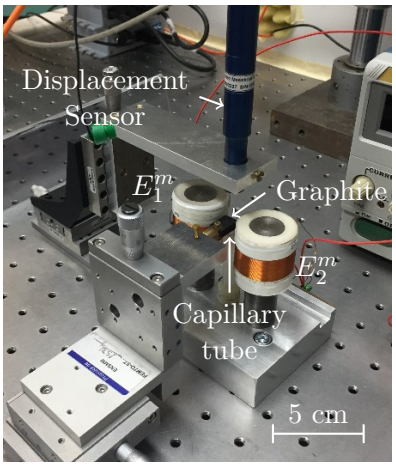

Fig. 3. Micro and nanoforce sensor placed on an anti-vibration table

air. As the height of the diamagnetic plates is large, the diamagnetic force belongs to the horizontal plan $(\boldsymbol{O}, \boldsymbol{x}, \boldsymbol{y})$, therefore it is not involved (Oster, 2012). The stable dynamics of the levitating tube along axis $\boldsymbol{z}$ is given by:

$$m\ddot{z} = -k_v\dot{z} + F_{elec} - mg + F_d \tag{3}$$

where z is the altitude of the levitating tube, m is its mass and k_v is the viscous damping coefficient due to the air friction against the tube and the magnet M.

The electromagnetic force F_{elec} depends on both the current i and the altitude z of the capillary tube. Modeling it over a wide range of altitudes can be done using finite element methods in order to take into account the iron core of the coils. Nevertheless, the altitude of the capillary tube is going to be regulated at a given reference altitude in the future. Thus a simple but realistic enough analytical expression of F_{elec} is necessary to design the observer and the state-space feedback controller. In this paper, only the observer is studied.

At the reference altitude, F_{elec} is directly proportional to the current i. Around that reference altitude, with sufficiently small displacements in $\boldsymbol{z}$, a linear variation of z can be considered as a first approximation. This leads to the following nonlinear modeling:

$$F_{elec} = (i_0 + i)(\gamma z + \beta) \tag{4}$$

where i_0 is the current value required to compensate the weight of the capillary tube and making it levitating in a steady state at a given altitude that is set to $z = 0$ by convention. The current i represents the current variation that will induce another stable altitude z_1 when the new steady state is reached above or below $z = 0$. The parameters γ and β are constant. They are identified from the experimental measurements around different operating points $O^{(i,z)}$ associated to any stable levitation position where the weight of the levitating tube is compensated for (see figure 2). In this steady state case, we have $F_{elec} = mg$ when no external force F_d is applied (see equation (3)).

The initial operating point $O^{(i_0,0)}$ is associated to the initial position, i.e the altitude $z = 0$, therefore (4) is equivalent to

$$F^0_{elec} = i_0\beta = mg. \tag{5}$$

From (5), the value of β is given by:

$$\beta = \frac{mg}{i_0}. \tag{6}$$

On the second stable operating point $O^{(i_1,z_1)}$ (chosen very close to $O^{(i_0,0)}$, as shown in figure 2), the altitude is z_1 and the current is $i_1 = i_0 + i$. Then (4) is equivalent to:

$$F^1_{elec} = (i_0 + i)(\gamma z_1 + \beta) = mg. \tag{7}$$

The parameter γ is then identified using (6) and (7):

$$\gamma = \frac{-i\beta}{z_1(i_0 + i)} < 0. \tag{8}$$

According to (4) and (6), the dynamics of the levitating tube (3) is equivalent to:

$$m\ddot{z} = -k_v\dot{z} + \gamma i_0 z + f_{elec} + F_d \tag{9}$$

where $f_{elec} = i(\gamma z + \beta)$ represents the force control input.

Equation (9) represents the dynamics of the capillary tube in active mode. In passive mode, the mode presented in this paper, there is no current variation, thus $i = 0$ and its dynamics is equivalent to:

$$m\ddot{z} = -k_v\dot{z} + \gamma i_0 z + F_d. \tag{10}$$

Equation (10) can be presented by the following state-space representation

$$\begin{cases} \dot{X} = AX + BF_d \\ y = CX + v \end{cases} \tag{11}$$

where $X = [x_1 \ x_2]^T = [z \ \dot{z}]^T$ and F_d represent respectively the state and the unknown external force to be estimated. The term v represents the noise affecting the displacement measurement and A, B and C are given by:

$$A = \begin{bmatrix} 0 & 1 \\ \frac{\gamma i_0}{m} & -\frac{k_v}{m} \end{bmatrix}, \quad B = \begin{bmatrix} 0 \\ \frac{1}{m} \end{bmatrix}, \quad C = [1 \ 0]. \tag{12}$$

4. INTERVAL OBSERVER DESIGN FOR STATE AND UNKNOWN EXTERNAL FORCE ESTIMATION

In this section an interval observer based on a Generic Linear Extended State Observer (GeLESO) is presented to estimate the state X and the unknown external force F_d in (11). The main idea of the GeLESO proposed by

Amokrane et al. (2019) is based on the definition of an extended state that includes the unknown external force. Therefore, the problem of state and unknown force estimation is transformed into a problem of state estimation only. Following the procedure given by Amokrane et al. (2019), the extended state component including the unknown external force F_d is given by:

$$x_3 = \frac{\gamma i_0}{m} x_1 + \frac{1}{m} F_d \tag{13}$$

such that (11) can be written as:

$$\begin{cases} \dot{X}^e = A_e X^e + B_e \dot{F}_d \\ y = C_e X^e + v \end{cases} \tag{14}$$

where $X^e = [\, x_1 \;\; x_2 \;\; x_3 \,]$ is the extended state vector to be estimated and where A_e, B_e and C_e read as:

$$A_e = \begin{bmatrix} 0 & 1 & 0 \\ 0 & -\frac{k_v}{m} & 1 \\ 0 & \frac{\gamma i_0}{m} & 0 \end{bmatrix}, \quad B_e = \begin{bmatrix} 0 \\ 0 \\ \frac{1}{m} \end{bmatrix}, \quad C_e = [1 \; 0 \; 0]\,. \tag{15}$$

The design of the interval observer for (14) requires the following assumptions:

Assumption 1. There exist some constants $\overline{v}$ and $\underline{v}$ such that $\underline{v} \leq v \leq \overline{v}$, and $\overline{v} = -\underline{v}$.

Assumption 2. The external force F_d is considered as a slowly time-varying disturbance, thus its derivative will be approximated by a null value.

According to Assumption 2, (14) becomes:

$$\begin{cases} \dot{X}^e = A_e X^e \\ y = C_e X^e + v. \end{cases} \tag{16}$$

The objective is now to find an upper and a lower bound for the external force F_d, the position z and the velocity $\dot{z}$ despite the unknown external force F_d and without any a priori knowledge on the bounds of the force dynamics, i.e. the bounds of $\dot{F}_d$. Since the force F_d is included in the extended state component (13), the reconstruction of the bounds for the position, the velocity and the force consists in the reconstruction of the bounds $\overline{X}^e$ and $\underline{X}^e$ for the extended state X^e. Note that an interval observer can be designed as a pair of two Luenberger-like observers, one for each bound.

Provided that Assumptions 1 and 2 are satisfied and according to Lemma 2 in section 2, the system

$$\begin{cases} \dot{\overline{X}}^e = (A_e - \mathcal{L}C_e)\overline{X}^e + \mathcal{L}y + |\mathcal{L}|\overline{v} \\ \dot{\underline{X}}^e = (A_e - \mathcal{L}C_e)\underline{X}^e + \mathcal{L}y + |\mathcal{L}|\underline{v} \end{cases} \tag{17}$$

is a possible interval observer for (16) if, for any initial condition $\underline{X}^e_0 \leq X^e_0 \leq \overline{X}^e_0$,

$$\underline{X}^e \leq X^e \leq \overline{X}^e, \quad \forall\, t \geq t_0. \tag{18}$$

Let $\overline{e} = \overline{X}^e - X^e$ be the upper estimation error and $\underline{e} = X^e - \underline{X}^e$ the lower one. Inequation (18) will be satisfied if, for any initial conditions $\overline{e}_0 = \overline{X}^e_0 - X^e_0 \geq 0$ and $\underline{e}_0 = X^e_0 - \underline{X}^e_0 \geq 0$, $\overline{e}$ and $\underline{e}$ are definite positive. The latter will be true if the dynamics of the upper and lower estimation errors, obtained from (16) and (17), fulfills the cooperativity condition, i.e. if

$$\begin{cases} \dot{\overline{e}} = (A_e - \mathcal{L}C_e)\overline{e} + \mathcal{L}v + |\mathcal{L}|\overline{v} \\ \dot{\underline{e}} = (A_e - \mathcal{L}C_e)\underline{e} - \mathcal{L}v - |\mathcal{L}|\underline{v} \end{cases} \tag{19}$$

is a cooperative system (see Lemma 2). As there is no gain vector $\mathcal{L}$ such that $A_e - \mathcal{L}C_e$ is a Metzler matrix, the system (19) is not cooperative, $\overline{e}$ and $\underline{e}$ are not definite positive $\forall\, t \geq 0$, and therefore the inequation (18) is not satisfied. As a consequence, the system (17) is not an interval observer for (16).

To guarantee that (19) is cooperative, $A_e - \mathcal{L}C_e$ can be transformed into a Metzler form using, for instance, a time-varying change of coordinates (Mazenc and Bernard, 2011) or a time-invariant one (Raissi et al., 2012). The latter is used in this paper. Its main idea is to find a nonsingular transformation matrix P, obtained by solving a Sylvester equation, such that $P(A_e - \mathcal{L}C_e)P^{-1}$ is Metzler.

In the new base with the new coordinates $\mathfrak{X} = PX^e$, the system (14) is transformed into:

$$\begin{cases} \dot{\mathfrak{X}} = PA_eP^{-1}\mathfrak{X} + PB_e\dot{F}_d \\ y = C_eP^{-1}\mathfrak{X} + v \end{cases} \tag{20}$$

which, according to Assumption 2, becomes:

$$\begin{cases} \dot{\mathfrak{X}} = PA_eP^{-1}\mathfrak{X} \\ y = C_eP^{-1}\mathfrak{X} + v \end{cases} \tag{21}$$

A candidate GeLESO-based interval observer for (21) is given by:

$$\begin{cases} \dot{\overline{\mathfrak{X}}} = P(A_e - \mathcal{L}C_e)P^{-1}\overline{\mathfrak{X}} + P\mathcal{L}y + |P\mathcal{L}|\overline{v} \\ \dot{\underline{\mathfrak{X}}} = P(A_e - \mathcal{L}C_e)P^{-1}\underline{\mathfrak{X}} + P\mathcal{L}y + |P\mathcal{L}|\underline{v} \end{cases} \tag{22}$$

where $P(A_e - \mathcal{L}C_e)P^{-1}$ is Metzler. The initial conditions of the bounds in the new base are calculated using Lemma 1 in section 2 and read as:

$$\begin{cases} \dot{\overline{\mathfrak{X}}}(0) = P^+\overline{x}_0 - P^-\underline{x}_0 \\ \dot{\underline{\mathfrak{X}}}(0) = P^+\underline{x}_0 - P^-\overline{x}_0 \end{cases} \tag{23}$$

where P is the solution of the following Sylvester equation (Raissi et al., 2012):

$$PA_e - RP = QC_e \tag{24}$$

where $Q = P\mathcal{L}$ and $R = P(A_e - \mathcal{L}C_e)P^{-1}$ (see Lemma 1 in (Raissi et al., 2012)).

Let $\overline{e} = \overline{\mathfrak{X}} - \mathfrak{X}$ be the upper estimation error and $\underline{e} = \mathfrak{X} - \underline{\mathfrak{X}}$ the lower one. Based on (21) and (22), the dynamics of the interval estimation errors is given by:

$$\begin{cases} \dot{\overline{e}} = P(A_e - \mathcal{L}C_e)P^{-1}\overline{e} + P\mathcal{L}v + |P\mathcal{L}|\overline{v} \\ \dot{\underline{e}} = P(A_e - \mathcal{L}C_e)P^{-1}\underline{e} - P\mathcal{L}v - |P\mathcal{L}|\underline{v} \end{cases} \tag{25}$$

Referring to Assumption 1, $P\mathcal{L}v + |P\mathcal{L}|\overline{v} \geq 0$ and $-P\mathcal{L}v - |P\mathcal{L}|\underline{v} = -P\mathcal{L}v + |P\mathcal{L}|\overline{v} \geq 0$, $\forall\, t \geq 0$. Consequently, as $P(A_e - \mathcal{L}C_e)P^{-1}$ is a Metzler matrix, the system (25) is cooperative. According to Lemma 2 in section 2, $\overline{e}$ and $\underline{e}$ are hence positive for any initial conditions $\overline{e}_0 = \overline{\mathfrak{X}} - \mathfrak{X} \geq 0$ and $\underline{e}_0 = \mathfrak{X} - \underline{\mathfrak{X}} \geq 0$. Thus, the upper bound $\overline{\mathfrak{X}}$ and the lower one $\underline{\mathfrak{X}}$ include the state $\mathfrak{X}$ at any time, i.e. $\underline{\mathfrak{X}} \leq \mathfrak{X} \leq \overline{\mathfrak{X}}$, $\forall\, t \geq 0$.

According to Lemma 1 in section 2, the upper bound $\overline{X}^e$ in the initial base and the lower one $\underline{X}^e$ are calculated using the following transformation:

$$\begin{cases} \overline{X}^e = M^+\overline{\mathfrak{X}} - M^-\underline{\mathfrak{X}} \\ \underline{X}^e = M^+\underline{\mathfrak{X}} - M^-\overline{\mathfrak{X}} \end{cases} \quad \text{with } M = P^{-1}. \tag{26}$$

Using (13) and (26), the upper bound and the lower bound of the unknown external force F_d are given by:

$$\begin{cases} \overline{F_d} = m\overline{\ddot{x}}_3 - \gamma i_0 \overline{x}_1 \\ \underline{F_d} = m\underline{\ddot{x}}_3 - \gamma i_0 \underline{x}_1 \end{cases} \quad (27)$$

5. EXPERIMENTAL RESULTS

The experimental setup is the one described in section 3. The current $i_0 = 0.17$ A is applied to compensate for the weight of the capillary tube. It ensures the levitation of the tube at a given altitude $z = 0$ by convention.

5.1 Parameters identification

Calibrating microforce sensors based on macroscopic seismic mass remains difficult due to the environmental factors like temperature, disturbances, vibrations, humidity, etc. Several dynamic calibration methods have been investigated. They are based on external force generation like impact force (Fujii and Fujimoto, 1999), step force (Fujii, 2003b) and oscillating force (Kumme, 1998; Fujii, 2003a). Since the mass m of the capillary tube is easily measured with a precision balance, the parameter β is determined using equation (6). The other parameters γ and K_v are identified using Prediction Error Methods (PEM) which is implemented in Matlab toolbox. All the identified and measured parameters values are given in Table 1.

Table 1. Nanoforce sensor parameters values

Parameter	m	β	γ	k_v
Value	$8,07.10^{-6}$	$4,66.10^{-4}$	$-0,0854$	$3,0418.10^{-6}$
Unit	kg	$kg.m/A.s^2$	$kg/A.s^2$	$N.s/m$

5.2 Model validation

To validate the model described in (10), one can compare its simulated response using the identified parameters in Table 1 and the physical measured displacement, when a known external force is applied (see next section). The two behaviors are shown in Figure 4 below and the matching between them is correct.

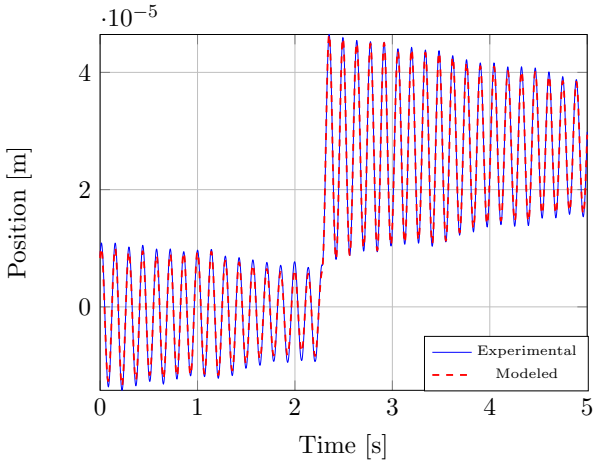

Fig. 4. Measured displacements of the capillary tube and the associated model response

5.3 Experimental validation of the interval observer

Applying the parameters values defined in Table 1 in the observer (17), it is impossible to find a gain vector $\mathcal{L}$ such that $A_e - \mathcal{L}C_e$ is Metzler. In this case, as explained in the previous section, a change of coordinates $\mathfrak{X} = PX^e$ must be used. The system (16) is then represented in the new base by (21). The numerical values of the matrices $A_e, \mathcal{L}, C_e$ and P are given by:

$$A_e = \begin{bmatrix} 0 & 1 & 0 \\ 0 & -0,4 & 1 \\ 0 & -1,799.10^3 & 0 \end{bmatrix}, \ \mathcal{L} = \begin{bmatrix} 300 \\ 25283 \\ 235072 \end{bmatrix}, \ C_e = [1\ 0\ 0]$$

$$P = \begin{bmatrix} 3,9508 & -0,0263 & 2,2644.10^{-4} \\ -2,9608 & 0,0258 & -2,2644.10^{-4} \\ 69,7181 & -0,7356 & 0,0106 \end{bmatrix}$$

which ensure that $P(A_e - \mathcal{L}C_e)P^{-1}$ is Metzler.

The gain vector $\mathcal{L}$ is calculated using a pole placement method as it is described in (Amokrane et al., 2019).

The upper and lower bounds of the measurement noise v, generated by the confocal chromatic sensor are quantified respectively to $\overline{v} = 5.10^{-8}$ m and $\underline{v} = -5.10^{-8}$ m.

To verify the efficiency of the proposed interval observer, a known external force is applied to the force sensor using the coils. This force is given by $i(\gamma z + \beta)$ with the identified parameters γ and β and a given current i.

The results of the proposed interval observer are shown in Figures 5, 6 and 7 for the following initial conditions:

$$\overline{x}_0 = [\,1, 7.10^{-5} \quad 4.5.10^{-3} \quad 5.10^{-5}\,]^T,$$
$$\underline{x}_0 = [\,-1, 7.10^{-5} \quad -4.5.10^{-3} \quad -5.10^{-5}\,]^T.$$

The proposed interval observer provides the guaranteed bounds of the position z, the velocity $\dot{z}$ and the external force F_d, without any a priori knowledge of the bounds of the external force dynamics $\dot{F}_d$. One can see from these figures that the intervals width is tight and that the convergence time of the observer is very short despite different initial conditions from the ones of the measurements, i.e. the measured vertical displacements.

Note that, in Figures 5, 6 and 7, the plot labelled "Estimation" is the observation provided by the GeLESO proposed by Amokrane et al. (2019).

6. CONCLUSION

Nanoforce sensors based on diamagnetic levitation using auto-stabilized magnetic springs are known for their low resonant frequency, low stiffness and their linear behavior. Moreover, the mechanical part manufacturing is a low-cost processing that does not necessitate any complex machining. A novel design of micro and nanoforce sensor based on diamagnetic levitation is proposed in this paper. In this sensor the levitating tube, called capillary tube, represents the sensitive part of the sensor, and converts the unknown external force into a vertical displacement. This new design is a one direction sensor for forces ranging from 1 nN to 1 μN. An interval observer based on the Generic Linear Extended State Observer approach is proposed to reconstruct the bounds of the state and the ones of the unknown external force. The experimental results show the

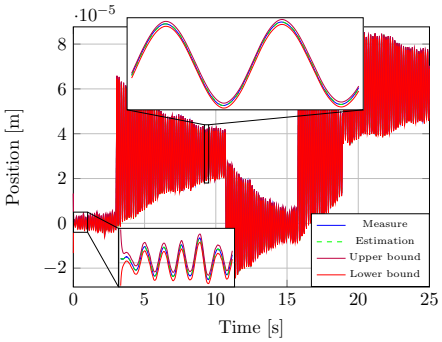

Fig. 5. Position z of the capillary tube

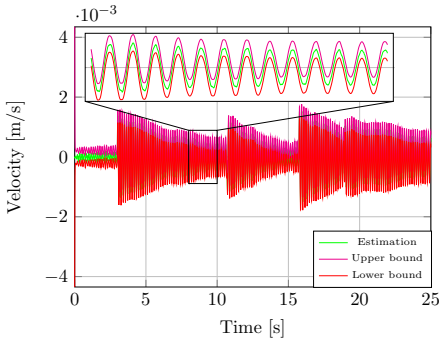

Fig. 6. Velocity $\dot{z}$ of the capillary tube

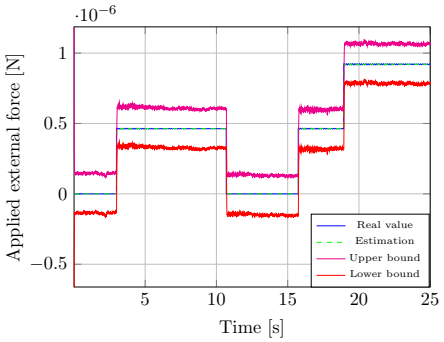

Fig. 7. External force $F_d = i(\gamma z + \beta)$

efficiency of the proposed interval observer. Future works will focus on the active mode, where a controller will be used to keep the capillary tube in its null position (zero displacement sensor). Furthermore, all the uncertainties (mass, current, measurement of displacement, identified parameters) will have to be taken into account to ensure a global measurement that fits into the metrology requirements.

ACKNOWLEDGEMENTS

This work has been supported by the EIPHI Graduate school (contract "ANR-17-EURE-0002")

REFERENCES

Amokrane, F., Piat, E., Abadie, J., Drouot, A., and Escareno, J. (2019). State observation of unknown nonlinear SISO systems based on virtual input estimation. *International Journal of Control*, 1–14.

Beyeler, F., Muntwyler, S., and Nelson, B. (2009). A Six-Axis MEMS Force–Torque Sensor With Micro-Newton and Nano-Newtonmeter Resolution. *Journal of Microelectromechanical Systems*, 18(2), 433–441.

Billot, M., Piat, E., Abadie, J., Agnus, J., and Stempflé, P. (2016). External mechanical disturbances compensation with a passive differential measurement principle in nanoforce sensing using diamagnetic levitation. *Sensors and Actuators A: Physical*, 238, 266–275.

Billot, M., Xu, X., Agnus, J., Piat, E., and Stempflé, P. (2015). Multi-axis MEMS force sensor for measuring friction components involved in dexterous micromanipulation: design and optimisation. *International Journal of Nanomanufacturing*, 11(3/4), 161.

Boukallel, M., Abadie, J., and Piat, E. (2003). Levitated micro-nano force sensor using diamagnetic materials. In *2003 IEEE International Conference on Robotics and Automation*. IEEE.

Chambon, E., Apkarian, P., and Burlion, L. (2015). Metzler Matrix Transform Determination using a Nonsmooth Optimization Technique with an Application to Interval Observers. In *2015 Proceedings of the Conference on Control and its Applications*, 205–211. Society for Industrial and Applied Mathematics.

Cherry, A., Abadie, J., and Piat, E. (2011). Analysis of a passive microforce sensor based on magnetic springs and upthrust buoyancy. *Sensors and Actuators A: Physical*, 169(1), 27–36.

Efimov, D., Fridman, L., Raïssi, T., Zolghadri, A., and Seydou, R. (2012). Interval estimation for LPV systems applying high order sliding mode techniques. *Automatica*, 48(9), 2365–2371.

Estevez, P., Bank, J., Porta, M., Wei, J., Sarro, P., Tichem, M., and Staufer, U. (2012). 6 DOF force and torque sensor for micro-manipulation applications. *Sensors and Actuators A: Physical*, 186, 86–93.

Fujii, Y. (2003a). A method for calibrating force transducers against oscillation force. *Measurement Science and Technology*, 14(8), 1259–1264.

Fujii, Y. (2003b). Proposal for a step response evaluation method for force transducers. *Measurement Science and Technology*, 14(10), 1741–1746.

Fujii, Y. and Fujimoto, H. (1999). Proposal for an impulse response evaluation method for force transducers. *Measurement Science and Technology*, 10(4), N31–N33.

Gana, R., Abadie, J., Piat, E., Roux, C., Amiot, C., Pieralli, C., and Wacogne, B. (2017). A novel force sensing platform using passive magnetic springs for mechanical characterisation of human oocytes. *Sensors and Actuators A: Physical*, 262, 114–122.

Gouzé, J., Rapaport, A., and Hadj-Sadok, M. (2000). Interval observers for uncertain biological systems. *Ecological Modelling*, 133(1-2), 45–56.

Hou, M. and Muller, P. (1992). Design of observers for linear systems with unknown inputs. *IEEE Transactions on Automatic Control*, 37(6), 871–875.

Kumme, R. (1998). Investigation of the comparison method for the dynamic calibration of force transducers. *Measurement*, 23(4), 239–245.

Mazenc, F. and Bernard, O. (2011). Interval observers for linear time-invariant systems with disturbances. *Automatica*, 47(1), 140–147.

Oster, S. (2012). Etude et réalisation d'un prototype avancé de plateforme de mesure de micro et nanoforce par lévitation diamagnétique. http://www.theses.fr/fr/177393270.

Piat, E., Abadie, J., and Oster, S. (2012). Nanoforce estimation based on Kalman filtering and applied to a force sensor using diamagnetic levitation. *Sensors and Actuators A: Physical*, 179, 223–236.

Raissi, T., Efimov, D., and Zolghadri, A. (2012). Interval State Estimation for a Class of Nonlinear Systems. *IEEE Transactions on Automatic Control*, 57(1), 260–265.

Shen, Y., Xi, N., and Li, W.J. (2003). Contact and force control in microassembly. In *Proceedings of the IEEE International Symposium on Assembly and Task Planning 2003*. IEEE.